ANL/RERTR/TM-11-21

# Computational Fluid Dynamics Analyses of Lateral Heat Conduction, Coolant Azimuthal Mixing and Heat Transfer Predictions in a BR2 Fuel Assembly Geometry

Nuclear Engineering Division

**About Argonne National Laboratory**
Argonne is a U.S. Department of Energy laboratory managed by UChicago Argonne, LLC under contract DE-AC02-06CH11357. The Laboratory's main facility is outside Chicago, at 9700 South Cass Avenue, Argonne, Illinois 60439. For information about Argonne and its pioneering science and technology programs, see www.anl.gov.

**Availability of This Report**
This report is available, at no cost, at http://www.osti.gov/bridge. It is also available on paper to the U.S. Department of Energy and its contractors, for a processing fee, from:

U.S. Department of Energy
Office of Scientific and Technical Information
P.O. Box 62
Oak Ridge, TN 37831-0062
phone (865) 576-8401
fax (865) 576-5728
reports@adonis.osti.gov

**Disclaimer**
This report was prepared as an account of work sponsored by an agency of the United States Government. Neither the United States Government nor any agency thereof, nor UChicago Argonne, LLC, nor any of their employees or officers, makes any warranty, express or implied, or assumes any legal liability or responsibility for the accuracy, completeness, or usefulness of any information, apparatus, product, or process disclosed, or represents that its use would not infringe privately owned rights. Reference herein to any specific commercial product, process, or service by trade name, trademark, manufacturer, or otherwise, does not necessarily constitute or imply its endorsement, recommendation, or favoring by the United States Government or any agency thereof. The views and opinions of document authors expressed herein do not necessarily state or reflect those of the United States Government or any agency thereof, Argonne National Laboratory, or UChicago Argonne, LLC.

ANL/RERTR/TM-11-21

# Computational Fluid Dynamics Analyses of Lateral Heat Conduction, Coolant Azimuthal Mixing and Heat Transfer Predictions in a BR2 Fuel Assembly Geometry

by
C.P. Tzanos and B. Dionne
Nuclear Engineering Division, Argonne National Laboratory

May 23, 2011

This work is sponsored by the
U.S. Department of Energy, National Nuclear Safety Administration (NNSA)
Office of Global Threat Reduction (NA-21)

## Table of Contents

I. Introduction ..... 4

II. Lateral Conduction and Azimuthal Coolant Mixing ..... 5
II.1. Analysis of lateral conduction in a typical BR2 fuel plate ..... 5
II.2. Azimuthal coolant mixing in a typical BR2 channel ..... 9
II.3. Analytical estimation of the impact of the azimuthal peaking ..... 10
II.4. Conclusions and summary ..... 11

III. Heat Transfer Predictions by CFD and Correlations in Pipe and Plate Geometries ..... 12
III.1. Computational approach ..... 13
III.2. Flow in a pipe ..... 14
III.3. Flow between plates ..... 19
III.4. Summary and conclusions ..... 23

References ..... 24

# I. Introduction

To support the analyses related to the conversion of the BR2 core from highly-enriched (HEU) to low-enriched (LEU) fuel, the thermal-hydraulics codes PLTEMP [1] and RELAP-3D [2] are used to evaluate the safety margins during steady-state operation (PLTEMP), as well as after a loss-of-flow, loss-of-pressure, or a loss of coolant event (RELAP).

In the 1-D PLTEMP and RELAP simulations, conduction in the azimuthal and axial directions is not accounted. The very good thermal conductivity of the cladding and the fuel meat and significant temperature gradients in the lateral directions (axial and azimuthal directions) could lead to a heat flux distribution that is significantly different than the power distribution. To evaluate the significance of the lateral heat conduction, 3-D computational fluid dynamics (CFD) simulations, using the CFD code STAR-CD [3], were performed.

Safety margin calculations are typically performed for a hot stripe, i.e., an azimuthal region of the fuel plates/coolant channel containing the power peak. In a RELAP model, for example, a channel between two plates could be divided into a number of RELAP channels (stripes) in the azimuthal direction. In a PLTEMP model, the effect of azimuthal power peaking could be taken into account by using engineering factors. However, if the thermal mixing in the azimuthal direction of a coolant channel is significant, a stripping approach could be overly conservative by not taking into account this mixing. STAR-CD simulations were also performed to study the thermal mixing in the coolant.

Section II of this document presents the results of the analyses of the lateral heat conduction and azimuthal thermal mixing in a coolant channel.

Finally, PLTEMP and RELAP simulations rely on the use of correlations to determine heat transfer coefficients. Previous analyses [4] showed that the Dittus-Boelter correlation gives significantly more conservative (lower) predictions than the correlations of Sieder-Tate and Petukhov. STAR-CD 3-D simulations were performed to compare heat transfer predictions from CFD and the correlations. Section III of this document presents the results of this analysis.

# II. Lateral Conduction and Azimuthal Coolant Mixing

To determine the significance of the lateral heat conduction (azimuthal and axial directions) and of thermal mixing, 3-D CFD simulations, which account for conduction (solids and fluid) and convection, were performed for steady-state and liquid-phase conditions in one channel of a BR2 fuel assembly. The operating conditions and power distribution reflect the core state at the initiation of the 1963 test A/400/1. The conclusions of this work are also applicable to fuel assemblies of the current BR2 core because they behave similarly. In the following discussion, "without conduction" means no conduction in the azimuthal and axial directions. Section II.1 presents the lateral heat conduction analyses; Section II.2 presents the analysis of the thermal mixing; and Section II.3 presents an analytical estimate of the impact of the azimuthal power peaking on peak cladding temperature at steady state.

## *II.1. Analysis of lateral conduction in a typical BR2 fuel plate*

In this analysis, for the simulation of turbulence the widely used standard high Reynolds (high-Re) number $k-\varepsilon$ model [3] was used. Flow in one half (symmetry) of one of the three sectors of a BR2 assembly between plates (full height-plate) five and six was considered. The simulated geometry includes two half-plates and one half of the stiffener section as shown in Fig. II-1. The height of the simulated domain is equal to the full height of a plate, i.e., 970 cm. With the exemption of the coolant inlet and outlet, all other boundaries were treated as adiabatic. A symmetry boundary condition was used at the flow symmetry boundary, and the boundary conditions at the inlet and outlet were: uniform inlet flow velocity of 11.8 m/s, inlet temperature of 35$^{o}$C, and outflow at the outlet.

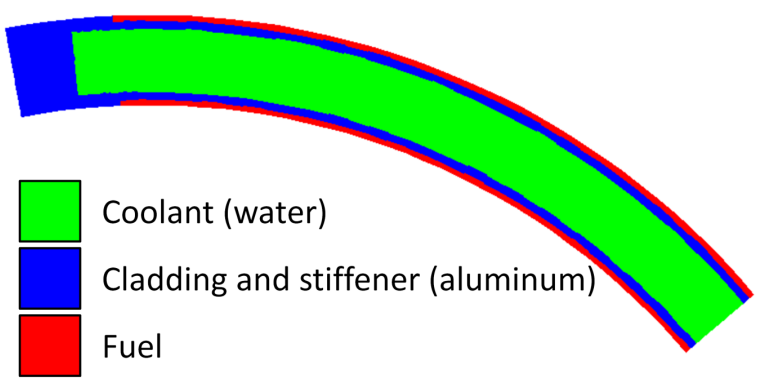


Figure II-1. Simulated geometry – high-Re model.

As in the current BR2 core, the BR2 fuel assemblies in the core of the 1963 tests were subjected to strong azimuthal power peaking. For this analysis, the expected worst azimuthal power distribution was determined from MCNP simulations of the 1963 core for test A/400/1 [5].

Specifically, a power distribution for plate 6 was calculated for 24 axial locations using 5 degrees azimuthal meshes. After inspection of the resulting distributions, it was found that the axial dependency of the azimuthal power shape could be approximated by two averaged distributions evaluated below and above 0.5612 m. An azimuthally-averaged axial power shape was also calculated. The power distribution is provided to STAR-CD by local-to-average axial and azimuthal polynomial functions calculated from the above power distributions. For simplicity, the polynomial functions shown in Figs. II-2 and II-3 are applied to both plates five and six.

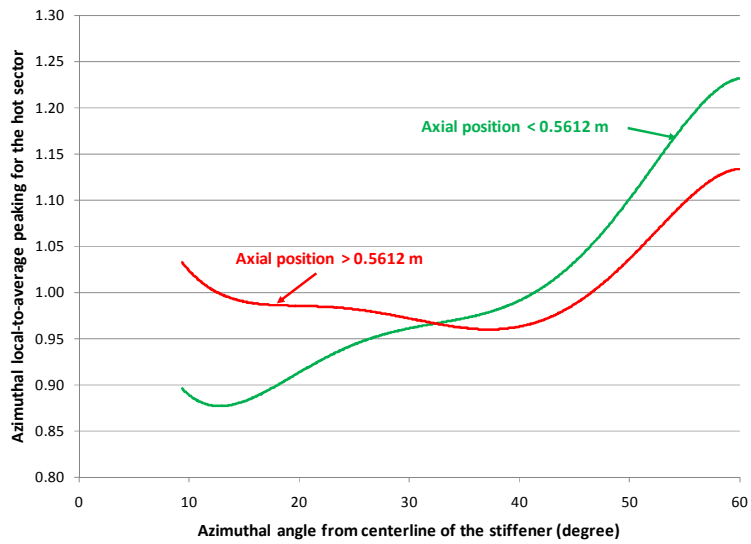


Figure II-2. Azimuthal power distibution.

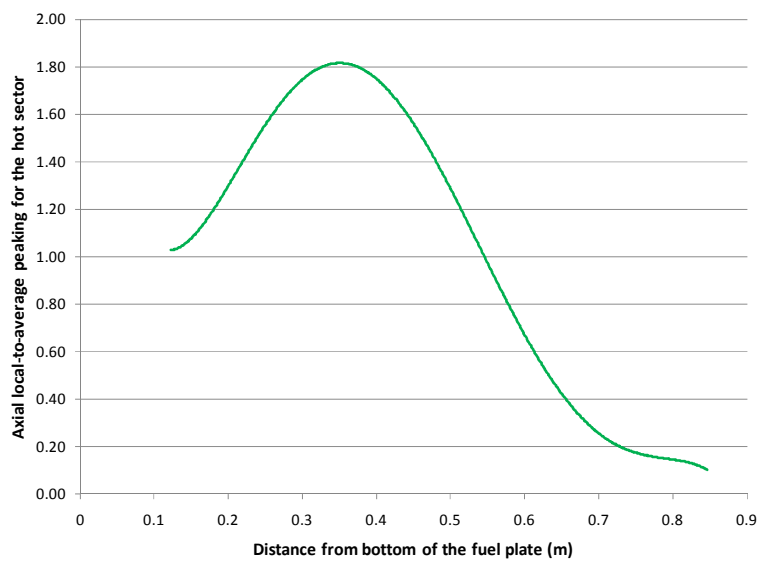


Figure II-3. Axial Power distribution.

The power density is evaluated from

$$Q_j(\theta, z) = q_j \, p_i(\theta) \, p(z) \,, \tag{II-1}$$

where $Q_j(\theta, z)$ is the power density (W/m$^3$) in plate 5 ($j$=5) and plate 6 ($j$=6), $q_j$ is the plate average power density (W/m$^3$), $p_i(\theta)$ is the azimuthal local-to-average distribution ($i$=1 below 0.5612 m, $i$=2 above 0.5612 m), and $p(z)$ is the axial local-to-average distribution.

Figure II-4 shows the azimuthal heat flux (to the coolant) distribution, with and without conduction in the fuel plate, in the fuelled section (fuel meat) of plate six at the elevation where the power density peaks (Fig. II-3). There is a very small reduction of the peak heat flux, and a more significant reduction, due to conduction to the stiffener, in a small portion of the fuelled section (about 15% of the total length in the azimuthal direction) that is adjacent to the aluminum stiffener. At the end (azimuthal edge) of the fuelled section, because of conduction, the heat flux drops to 40% of its value without conduction.

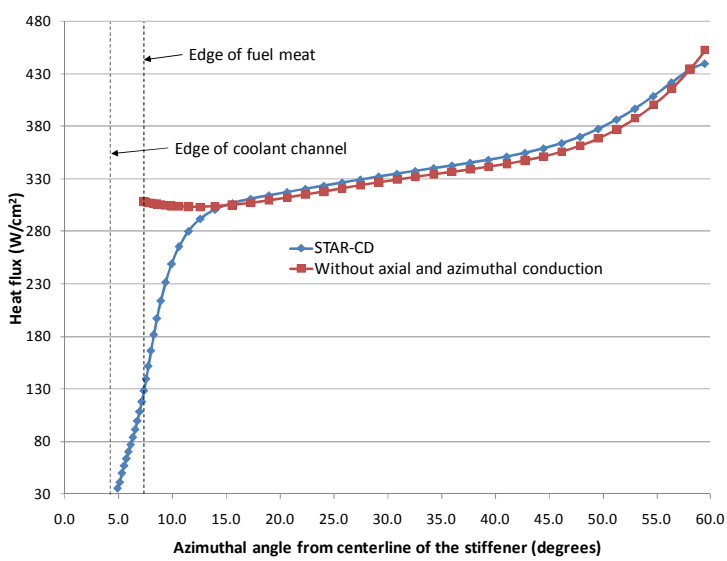


Figure II-4. Azimuthal heat flux distribution at 0.333m from the bottom of the plate.

The total heat transferred by conduction out of the fuelled section of the plate in the azimuthal direction is 2.9% of the total heat generated in the plate. The heat transferred by axial conduction out of the fuelled section of the plate to the outlet aluminum section of the plate is less than 0.2%, and that to the inlet aluminum section of the plate is about one tenth of this.

Figure II-5 shows the azimuthal cladding temperature distribution at the elevation of the peak power density with the power density varying in the azimuthal and axial directions, as well as with the power distribution varying only in the axial direction. In the first case, it drops from 91.8 °C at the center of the plate to 58.5 °C at the end (azimuthal direction) of the fuel meat. In the second case, it peaks at 80.6 °C.

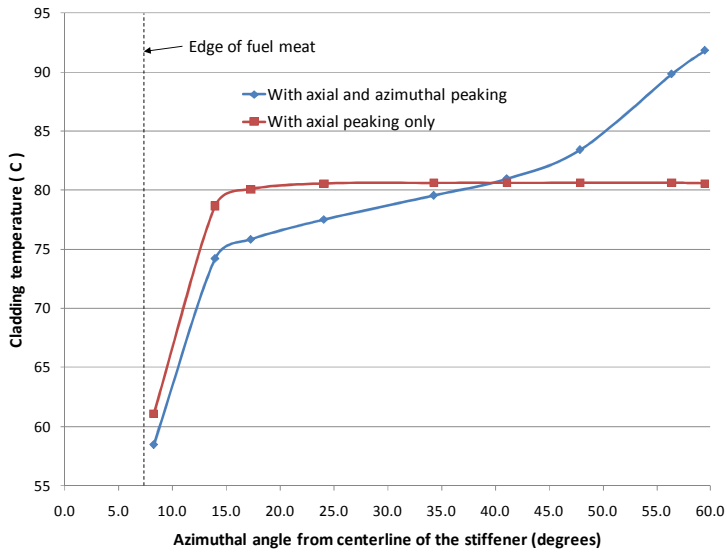


Figure II-5. Azimuthal cladding temperature distribution.

Figure II-6 shows the coolant temperature distribution at the elevation of the peak power density, and Fig. II-7 shows the same variable at the channel outlet.

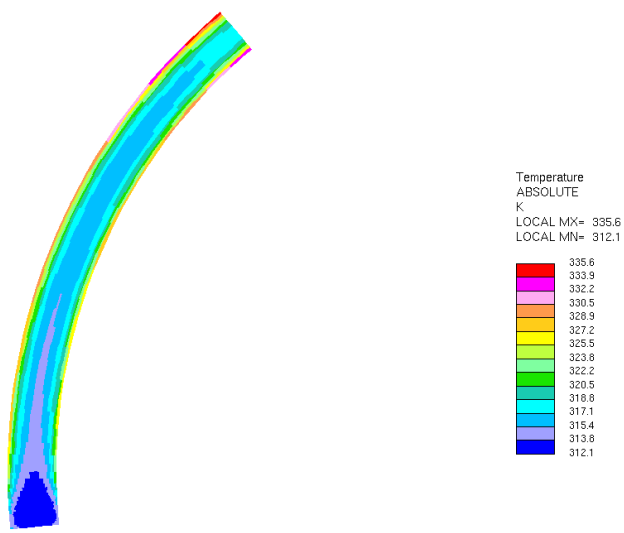


Figure II-6. Coolant temperature distribution at the elevation of peak power density.

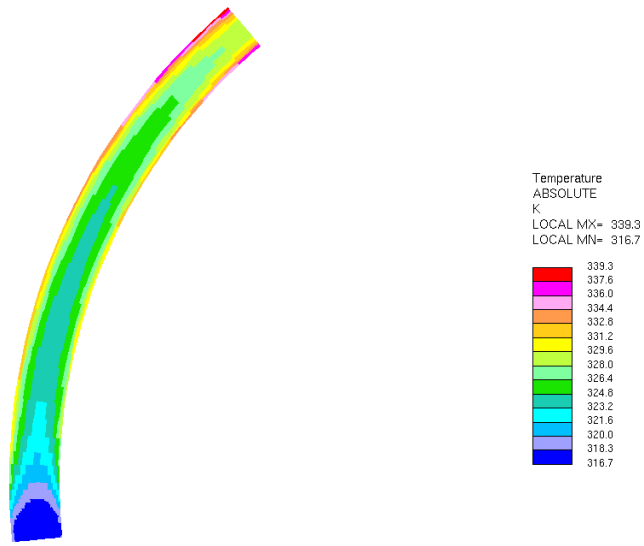


Figure II-7. Coolant temperature distribution at channel outlet.

The azimuthal variation of the power distribution leads to an azimuthal variation in coolant temperature which can promote thermal mixing in the same direction.

## *II.2. Azimuthal coolant mixing in a typical BR2 channel*

To assess the significance of azimuthal mixing, a CFD simulation was performed with the azimuthal power density variation as shown in Fig. II-2, but, for simplicity, with a uniform axial power distribution. This simplification has no significant effect on the conclusions of this analysis on thermal mixing in the azimuthal direction. The total power in the plates was kept the same as in the case of the actual axial power distribution. Figure II.8 shows the azimuthal distribution of the coolant temperature rise at the channel outlet, and the same distribution resulting from

$$\Delta T(\theta) = q(\theta)/ [m(\theta)C_p], \qquad \text{(II-2)}$$

where:

$\Delta T(\theta)$ = Temperature rise from inlet to outlet at a stripe (sector) of size $\Delta\theta$ at angle $\theta$
$q(\theta)$ = Heat transferred to the coolant at the above stripe (computed from the CFD simulation)
$m(\theta)$ = Flow rate at the stripe (computed from the CFD simulation)
$C_p$ = Specific heat

Figure II-8 shows that thermal mixing in the azimuthal direction is minimal. It reduces the peak temperature rise by 1 °C, and the temperature rise at the fuel edge by 2 °C. Thus, using striping in RELAP and PLTEMP simulations is a good approximation, at least at steady state.

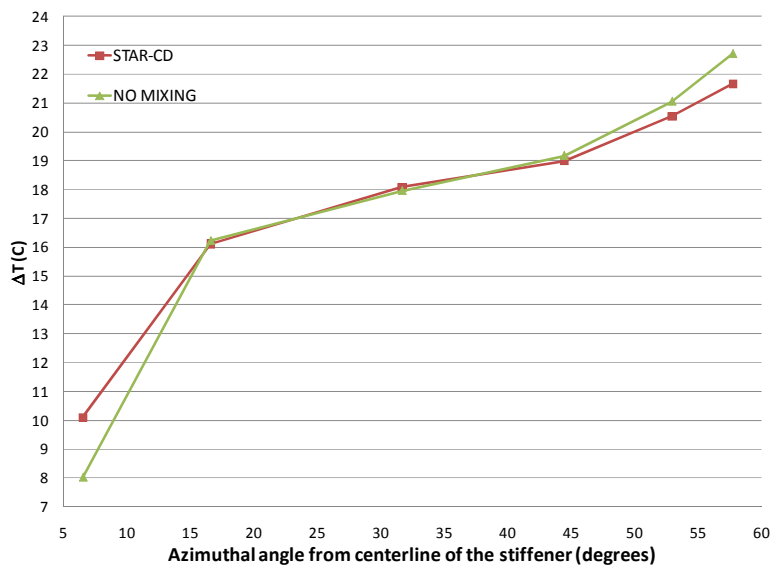


Figure II-8. Azimuthal distribution of coolant temperature rise (inlet to outlet).

Because striping is a good approximation, at steady-state the actual peak cladding temperature can be estimated analytically from the value determined from a thermal-hydraulic calculation (e.g., RELAP or PLTEMP) with averaging in the azimuthal direction (no striping).

## *II.3. Analytical estimation of the impact of the azimuthal peaking*

This section presents an analytical relationship for the estimation of the impact of azimuthal power peaking on the cladding temperature using results from an analysis of cladding temperatures where an average power distribution is used in the azimuthal direction.

If $p_a$ and $p_\theta$ are the peak to average power density ratios in the axial and azimuthal directions (power density varies in the axial and azimuthal direction), then the equations for heat transfer at the location of the peak power density give

*No azimuthal averaging:* $$qp_a p_\theta = h(T_c - T_f) \quad \text{(II-3)}$$

*Azimuthal averaging:* $$qp_a = h(T_{ca} - T_{fa}) \quad \text{(II-4)}$$

where $q$ is the plate average heat flux, $T_c$ and $T_f$ are the cladding and coolant temperatures when azimuthal variation of the power density is considered, and $T_{ca}$ and $T_{fa}$ are the cladding and coolant temperatures when azimutahal variation of the power density is not considered.

Assuming that the heat transfer coefficients are identical, Eqs II-3 and II-4 can be combined to obtain,

$$T_c = T_f + p_\theta (T_{ca} - T_{fa}) \quad \text{(II-5)}$$

From a heat balance in a stripe at the location of the peak power density and a stripe of average power density,

$$T_f - T_{in} = p_\theta (T_{fa} - T_{in}) \quad \text{(II-6)}$$

From Eqs II-5 and II-6,

$$T_c - T_{ca} = (p_\theta - 1)(T_{ca} - T_{in}) \quad \text{(II-7)}$$

In the analysis presented here, $T_{in}$ = 34.94 °C, $p_\theta$ =1.26 (average of distributions shown in Fig. II-2), and $T_{ca}$ = 80.6 °C (cladding temperature at the location of peak power density computed from a thermal-hydraulic analysis, e.g., CFD or RELAP or PLTEMP, where the power density has been averaged in the azimuthal direction). With these values, Eq. II-7 gives $T_c$ = 92.4 °C, which agrees well with the value of 91.8 °C computed by CFD without averaging in the azimuthal direction, and $T_c - T_{ca}$ = 11.8 °C. The difference $T_c - T_{ca}$ is an estimate of the difference $T_{cp}$ - $T_{cap}$ of the peak cladding temperatures computed without and with azimuthal averaging of the power distribution.

## II.4. Conclusions and summary

In summary, the CFD simulations presented here show that lateral (axial and azimuthal) conduction in the plate have no significant effect on the value of the peak heat flux from the plate to the coolant. Thermal mixing in the azimuthal direction is minimal, and the use of azimuthal stripping in RELAP or PLTEMP steady state analyses is a good approximation. This analysis also shows that azimuthal conduction is of significance in the section of the plate close to the aluminum stiffener. Thus, the most limiting power distribution is that where the power density peaks in the middle of the plate.

# III. Heat Transfer Predictions by CFD and Correlations in Pipe and Plate Geometries

In the thermal-hydraulic analyses performed for the safety analysis of BR2, the correlation of Sieder-Tate was used for the computation of the heat transfer coefficient. Preliminary thermal-hydraulic analyses performed recently [4] to determine safety margins to onset of nucleate boiling (ONB) for HEU and LEU fuel at BR2 have shown that the use of the Dittus-Boelter correlation for the heat transfer coefficient gives significantly more conservative (lower) predictions than the correlations of Sieder-Tate and Petukhov [6].

The above mentioned correlations are:

Dittus-Boelter:

$$Nu = 0.023\,\mathrm{Re}^{0.8}\,\mathrm{Pr}^{0.4} \tag{III-1}$$

Sieder-Tate

$$Nu = 0.027\,\mathrm{Re}^{0.8}\,\mathrm{Pr}^{1/3}\left(\frac{\mu_b}{\mu_w}\right)^{0.14} \tag{III-2}$$

Petukhov:

$$Nu / Nu_0 = \left(\mu_b / \mu_w\right)^{0.11}$$

$$Nu_0 = \frac{(f/8)\,\mathrm{Re}\,\mathrm{Pr}}{K_1(f) + K_2(\mathrm{Pr})(f/8)^{1/2}(\mathrm{Pr}^{2/3} - 1)}$$

$$f = (1.82\log\mathrm{Re} - 1.64)^{-2} \tag{III-3}$$

$$K_1(f) = 1 + 3.4f,\ \ K_2(\mathrm{Pr}) = 11.7 + 1.8\,\mathrm{Pr}^{-1/3}$$

Where

| | | |
|---|---|---|
| Nu | = | Nusselt number = $hd_h/k$ |
| Re | = | Reynolds number = $u\rho d_h/\mu$ |
| Pr | = | Prandtl number = $\frac{\mu C_p}{k}$ |
| $\mu$ | = | fluid viscosity |
| $C_p$ | = | fluid specific heat at constant pressure |
| $k$ | = | fluid thermal conductivity |
| $\rho$ | = | fluid density |
| $d_h$ | = | hydraulic diameter |
| $h$ | = | heat transfer coefficient |

In the correlation of Dittus-Boelter, all physical properties are evaluated at the bulk temperature of the fluid. In the other two correlations, $\mu_w$ is evaluated at the wall temperature and all other physical properties are also evaluated at the bulk temperature of the fluid. In the analysis presented here, another correlation was also considered designated as Dittus-Boelter-M. This correlation is similar to the Petukhov correlation with $Nu_0$ computed from the Dittus-Boelter correlation.

Reference [6] used experimental data of heat transfer in pipes, to show that the exponent of the viscosity ratio $\mu_w / \mu_b$ should be 0.11 when the fluid is heated, instead of 0.14 used in the Sieder-Tate correlation. This data covers Reynolds (Re) number values varying from 5000 to 123000, Prandtl number varying from 2 to 140, and $\mu_w / \mu_b$ ratios varying from .08 to one, For temperatures close to the boiling point the viscosity of water varies very significantly from the center of a channel to the cladding surface of the fuel plate. Thus, in safety margin evaluations (OB, ONB) accounting for the effect of this variation on the heat transfer coefficient can be of significance.

In CFD simulations, the heat transfer is computed by using the conductivity of the fluid and the turbulent conductivity resulting from the turbulence model. Many RANS (Reynolds Averaged Navier-Stokes) models of turbulence have been presented in the literature, but none of them is of universal applicability. The low Reynolds (low-Re) number $k-\varepsilon$ models and the v2f model resolve the boundary layer, and do not use the "logarithmic wall function" approximation. Because these models resolve the boundary layer, it seems that they should be more appropriate for flows where the fluid properties vary significantly from the "bulk" of the fluid to the wall (especially in the area close to the wall), as the case is in water for temperatures close to the boiling point.

The correlations mentioned above were developed for flow in a pipe. To support the selection of the proper heat transfer correlation for the analysis of determining the margin to OB or ONB a CFD analysis of the heat transfer to water under conditions close to boiling was undertaken: (a) for flow in a pipe, and (b) for flow in a BR2 two-plate geometry.

## *III.1. Computational approach*

In this CFD analysis, simulations were performed with the standard high Reynolds (high-Re) number $k-\varepsilon$ model [3], the standard low-Re model [3], and the v2f model of turbulence [3]. Because the Dittus-Boelter correlation does not account for the variation of viscosity from the bulk temperature to the wall temperature, for pipe flow, CFD simulations were performed with variable fluid properties and with constant (artificially) properties. The latter case is also an approximation to the conditions prevailing at low heat fluxes.

In this analysis, the Re number was varied from about 66000 to about 300000, with wall temperatures close to the boiling point in the region close to the outlet of the flow domain. These Re number values cover the range of values computed in the preliminary BR2 analyses of Ref. [4]. The heat transfer coefficients reported here were computed near the bottom of the fuelled

section of the plate where the flow was well developed, and the wall temperature was close to the boiling point.

## *III.2. Flow in a pipe*

### III.2.1. Low-Re and v2f models

The numerical test problems analyzed here use heat transfer to water in a pipe having a diameter of 0.0331m, a heated length of 3.0m preceded by an unheated section of .75m (22 diameters). This is the pipe used in the experiments of Ref. [7] for heat transfer in a range of heat fluxes and Re numbers where buoyancy effects are significant. In the analyses presented here heat fluxes on the wall and flow rates (Re number) were used that cover the conditions relevant to an OB or ONB analysis for BR2. A water temperature of 40$^o$C was used at the pipe inlet and temperature dependent water properties were used at a pressure of 1.2 MPa.

Because the CFD models considered here resolve the boundary layer, the center of the computational cells next to the wall was located at a non-dimensional distance of about one y+ [8] from the wall. The heat transfer from the wall to a fluid cell next to the wall was computed from

$$q = k\,(T_w - T_c)/d \qquad \text{(III-4)}$$

where

| | | |
|---|---|---|
| $q$ | = | heat flux from the wall, |
| $T_w, T_c$ | = | wall and fluid cell temperature, and |
| $d$ | = | distance of cell center from the wall. |

The heat transfer coefficient $h$ was computed from

$$q = h\,(T_w - T_b) \qquad \text{(III-5)}$$

where $T_b$ is the bulk fluid temperature.

Table III-1 shows predictions of the heat transfer coefficient, $h$, for constant fluid properties (density, viscosity and specific heat at 27 $^o$C, viscosity was varied with Re number). To compare these predictions, the heat transfer coefficient computed from the Petukhov correlation, $h_p$, is used as a reference. At Re=66112, the low-Re model predicts the lowest heat transfer coefficient, 16% lower than $h_p$, while the prediction of the Dittus-Boelter correlation is 13% lower than $h_p$ . The prediction of the v2f model is smaller than that of the Petukhov correlation by less than 5%, while that of the Sieder-Tate is smaller by 9%.

Table III-1. Constant Properties

| Re = 66112, Pr = 5.8388 | | |
|---|---|---|
| Method | h | $h/h_p$ |
| v2f model | 6727 | 0.953 |
| Low-Re model | 5950 | 0.843 |
| Dittus – Boelter | 6172 | 0.874 |
| Sieder – Tate | 6441 | 0.912 |
| Petukhov | 7059 | |
| Re = 132224, Pr = 2.9194 | | |
| Method | h | $h/h_p$ |
| v2f model | 9634 | 1.072 |
| Low-Re model | 8890 | 0.990 |
| Dittus – Boelter | 8144 | 0.907 |
| Sieder – Tate | 8901 | 0.991 |
| Petukhov | 8983 | |
| Re = 198359, Pr = 1.9460 | | |
| Method | h | $h/h_p$ |
| v2f model | 11662 | 1.155 |
| Low-Re model | 12214 | 1.210 |
| Dittus – Boelter | 9578 | 0.949 |
| Sieder – Tate | 10756 | 1.065 |
| Petukhov | 10093 | |

At Re=132224, the Dittus-Boelter correlation gives the lowest $h$ value, 9% lower than $h_p$. The predictions of the Sieder-Tate correlation and of the low-Re model are lower than $h_p$ by only 1%, while the prediction of the v2f model is 7% higher than $h_p$ .

At Re=198359, the Dittus-Boelter correlation gives again the lowest prediction, 5% lower than $h_p$ .The prediction of the Sieder-Tate correlation is 6% higher than $h_p$, while the predictions of the CFD models are significantly higher; of the v2f model by 15% and of the low-Re model by 21%.

Table III-2 shows predictions of the heat transfer coefficient, $h$, for variable fluid properties.

At Re equal to about 67000, the Dittus-Boelter correlation and the low-Re model predict the lowest values; they are 12% and 10%, respectively, lower than $h_p$. The modified Dittus-Boelter correlation predicts a value 6% lower than $h_p$, while the Sieder-Tate correlation predicts a value 6% higher than $h_p$.

Table III-2. Variable Properties

| Re = 67344, Pr = 2.5845, $\mu_w/\mu_b$ = 0.533 | | | Re = 67344, Pr = 2.5845, $\mu_w/\mu_b$ = 0.565 | | |
|---|---|---|---|---|---|
| Method | h | $h/h_p$ | Method | h | $h/h_p$ |
| Low-Re | 5031 | 0.904 | v2f | 5676 | 1.027 |
| Dittus – Boelter | 4886 | 0.878 | Dittus – Boelter | 4886 | 0.884 |
| Dittus – Boelter-M | 5236 | 0.941 | Dittus – Boelter-M | 5203 | 0.941 |
| Sieder – Tate | 5879 | 1.057 | Sieder – Tate | 5831 | 1.054 |
| Petukhov | 5564 | | Petukhov | 5528 | |
| Re = 83077, Pr = 2.0596, $\mu_w/\mu_b$ = 0.460 | | | Re = 83079, Pr = 2.0596, $\mu_w/\mu_b$ = 0.469 | | |
| Low-Re | 6338 | 1.045 | v2f | 6558 | 1.083 |
| Dittus – Boelter | 5368 | 0.885 | Dittus – Boelter | 5368 | 0.887 |
| Dittus – Boelter-M | 5847 | 0.964 | Dittus – Boelter-M | 5835 | 0.964 |
| Sieder – Tate | 6695 | 1.104 | Sieder – Tate | 6677 | 1.103 |
| Petukhov | 6066 | | Petukhov | 6053 | |
| Re = 138671, Pr = 2.4757, $\mu_w/\mu_b$ = 0.416 | | | Re = 139904, Pr = 2.4757, $\mu_w/\mu_b$ = 0.410 | | |
| Low-Re | 12402 | 1.202 | v2f | 12122 | 1.174 |
| Dittus – Boelter | 8662 | 0.840 | Dittus – Boelter | 8662 | 0.839 |
| Dittus – Boelter-M | 9540 | 0.925 | Dittus – Boelter-M | 9555 | 0.925 |
| Sieder – Tate | 10824 | 1.050 | Sieder – Tate | 10845 | 1.050 |
| Petukhov | 10314 | | Petukhov | 10329 | |
| Re = 166150, Pr = 2.0596, $\mu_w/\mu_b$ = 0.464 | | | Re = 166156, Pr = 2.0595 $\mu_w/\mu_b$ = 0.463 | | |
| Low-Re | 12875 | 1.197 | v2f | 12816 | 1.191 |
| Dittus – Boelter | 9346 | 0.869 | Dittus – Boelter | 9347 | 0.868 |
| Dittus – Boelter-M | 10170 | 0.946 | Dittus – Boelter-M | 10174 | 0.946 |
| Sieder – Tate | 11643 | 1.083 | Sieder – Tate | 11647 | 1.083 |
| Petukhov | 10755 | | Petukhov | 10758 | |
| Re = 207720, Pr = 2.0596, $\mu_w/\mu_b$ = 0.505 | | | Re = 207726, Pr = 1.9824 $\mu_w/\mu_b$ = 0.463 | | |
| Low-Re | 14602 | 1.161 | v2f | 15010 | 1.195 |
| Dittus – Boelter | 11021 | 0.876 | Dittus – Boelter | 11022 | 0.877 |
| Dittus – Boelter-M | 11883 | 0.945 | Dittus – Boelter-M | 11866 | 0.945 |
| Sieder – Tate | 13604 | 1.081 | Sieder – Tate | 13579 | 1.081 |
| Petukhov | 12581 | | Petukhov | 12562 | |

At Re equal to about 83080, the lowest $h$ value is predicted by the Dittus-Boelter correlation, 11% lower than $h_p$. The prediction of the modified Dittus-Boelter correlation is 4% lower than $h_p$, while the Sieder-Tate correlation predicts a value 10% higher than $h_p$. The low-Re model predicts a heat transfer coefficient value 5% higher than $h_p$, while the v2f model predicts a value 8% higher.

At Re equal to about 166150, the Dittus-Boelter correlation predicts the lowest value, 13% lower than $h_p$. The prediction of the modified Dittus-Boelter correlation is 5% lower than $h_p$, while the Sieder-Tate correlation predicts a value 8% higher than $h_p$. Both CFD models predict a heat transfer coefficient value about 19% higher than $h_p$.

Reference [8] has compared predictions of the Sieder-Tate and Petukhov correlations with experimental data for Re values from 10000 to 100000 and $\mu_w/\mu_b$ ratios varying from 0.347 to 0.699. On the average, the Sieder-Tate correlation overpredicts the Nu number by 23%, while the average deviation of the predictions of the Petukhov correlation from the experimental data is 4.1%. For constant fluid properties and the same range of Re values, Ref. [8] found that the average deviation of predictions from the experimental data is 14% (mostly overprediction) for the Dittus-Boelter correlation and 4.1 % for the Petukhov correlation. The experimental data had a maximum spread of about 15%.

### III.2.2. Standard high Reynolds number $k-\varepsilon$ model

In the analyses with the high-Re model, heat transfer to water in a pipe having a diameter of 0.01058 m, and a heated length of 0.5 m (about 47 hydraulic diameters) was considered. A different pipe was used in this analysis because the CFD grid structure for this pipe was available (it had also been used in some other CFD analyses). As in the analysis presented in the previous section, heat fluxes on the wall and flow rates (Re number) were used that cover the conditions relevant to an OB or ONB analysis for BR2. A water temperature of 40 $^{o}$C was used at the pipe inlet and temperature dependent water properties were used at a pressure of 1.2 MPa.

In simulations with the high-Re model, the distance from the wall of the center of the computational cells adjacent to a wall must be between about 30 and 100 y+. In the analyses presented here this constraint was satisfied. The high-Re model, which does not resolve the boundary layer, computes the heat transfer from the wall to a fluid cell next to the wall from

$$q = h_w (T_w - T_c) \qquad \text{(III-6)}$$

where

$q$ = heat flux from the wall,
$h_w$ = heat transfer coefficient computed by the model, and
$T_w, T_c$ = wall and fluid cell temperature.

The heat transfer coefficient $h$ to be compared with that computed from the correlations was computed from

$$q = h_w (T_w - T_c) = h (T_w - T_b) \qquad \text{(III-7)}$$

where $T_b$ is the bulk fluid temperature.

Table III-3 shows predictions of the heat transfer coefficient, $h$, for constant fluid properties (all at T =27 $^{o}$C), and for Re number values varying fro 67000 to 200000. The Petukhov correlation predicts a higher heat transfer coefficient, $h_p$. The predictions of the high-Re model are consistently about 7% lower than $h_p$. The Dittus – Boelter correlation predicts the smallest value of $h$, which is up to 18% lower than $h_p$, and the discrepancy increases as the Re number

increases. The predictions of the Sieder-Tate correlation are up to 14% lower than $h_p$, and the discrepancy also increases as the Re number increases.

Table III-3. Constant Properties - High-Re model vs Correlations

| Re = 67001, Pr = 5.8388 | | |
|---|---|---|
| Method | h | $h/h_p$ |
| High-Re model | 20798 | 0.931 |
| Dittus – Boelter | 19523 | 0.874 |
| Sieder – Tate | 20374 | 0.912 |
| Petukhov | 22343 | |
| Re = 100009, Pr = 5.8388 | | |
| Method | h | $h/h_p$ |
| High-Re model | 29411 | 0.936 |
| Dittus – Boelter | 26897 | 0.856 |
| Sieder – Tate | 28070 | 0.894 |
| Petukhov | 31408 | |
| Re = 150018, Pr = 5.8388 | | |
| Method | h | $h/h_p$ |
| High-Re model | 41804 | 0.941 |
| Dittus – Boelter | 37204 | 0.837 |
| Sieder – Tate | 38827 | 0.874 |
| Petukhov | 44427 | |
| Re = 210027, Pr = 5.8388 | | |
| Method | h | $h/h_p$ |
| High-Re model | 55667 | 0.931 |
| Dittus – Boelter | 48696 | 0.821 |
| Sieder – Tate | 50820 | 0.857 |
| Petukhov | 59327 | |

Table III-4 shows predictions of the heat transfer coefficient, *h,* for variable fluid properties. The predictions of the high-Re model are consistently about 6% higher than $h_p$. The Dittus – Boelter correlation predicts the smallest value of *h,* which is up to 16% lower than $h_p$. The predictions of the modified Dittus – Boelter correlation are up to 8% lower than $h_p$ and those of the Sieder – Tate correlation are up to 9% higher than $h_p$.

Table III-4. Variable Properties - High-Re model vs Correlations

| Re = 70004, Pr = 2.3000, $\mu_w/\mu_b$ = 0.416 | | |
|---|---|---|
| Method | h | $h/h_p$ |
| High-Re model | 18498 | 1.050 |
| Dittus – Boelter | 15249 | 0.866 |
| Dittus – Boelter-M | 16791 | 0.954 |
| Sieder – Tate | 19143 | 1.087 |
| Petukhov | 17609 | |
| Re = 100007, Pr = 2.3000, $\mu_w/\mu_b$ = 0.416 | | |
| Method | h | $h/h_p$ |
| High-Re model | 24956 | 1.056 |
| Dittus – Boelter | 20284 | 0.858 |
| Dittus – Boelter-M | 22336 | 0.945 |
| Sieder – Tate | 25465 | 1.077 |
| Petukhov | 23642 | |
| Re = 150013, Pr = 2.3000, $\mu_w/\mu_b$ = 0.416 | | |
| Method | h | $h/h_p$ |
| High-Re model | 35100 | 1.060 |
| Dittus – Boelter | 28057 | 0.847 |
| Dittus – Boelter-M | 30895 | 0.933 |
| Sieder – Tate | 35222 | 1.063 |
| Petukhov | 33122 | |
| Re = 200025, Pr = 2.3000, $\mu_w/\mu_b$ = 0.416 | | |
| Method | h | $h/h_p$ |
| High-Re model | 44740 | 1.062 |
| Dittus – Boelter | 35318 | 0.838 |
| Dittus – Boelter-M | 38890 | 0.923 |
| Sieder – Tate | 44338 | 1.052 |
| Petukhov | 42132 | |

## *III.3. Flow between plates*

Flow in one of the three sectors of a BR2 assembly between plates (full height-plate) five and six was considered. Only half of the sector was simulated with a uniform power density in the fuelled part of the plate. Simulations were performed with the standard high Reynolds number $k-\varepsilon$ model and with the v2f model, and with variable properties only.

In the high-Re model simulations, the geometry included two half-plates and one half of the stiffener section as shown in Fig. III-1.

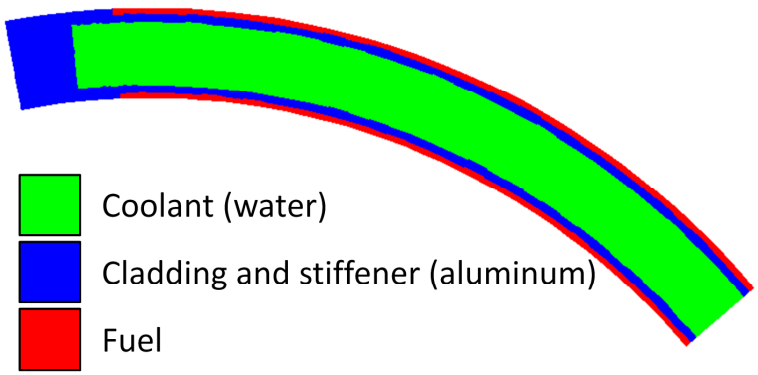


Figure III-1. Simulated geometry – high-Re model

With the v2f model, to avoid an excessive number of computational cells (this model resolves the boundary layer) only half of the channel between plates five and six was simulated as shown in Fig. III-2.

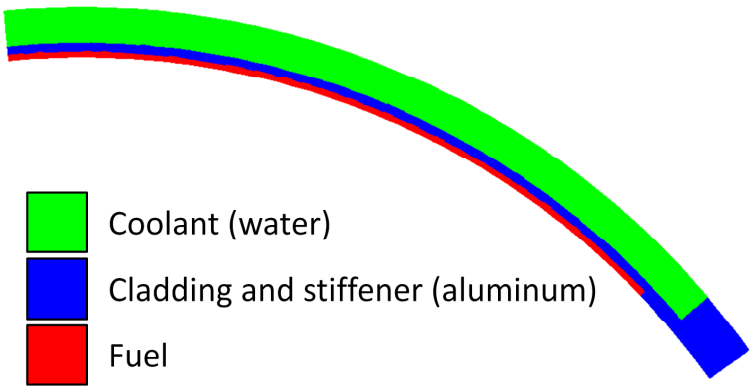


Figure III-2. Simulated geometry – v2f model

With the exemption of the coolant inlet and outlet, all other boundaries were treated as adiabatic. A symmetry boundary condition was used at boundaries of flow symmetry, and the boundary conditions at the inlet and outlet were: uniform inlet flow velocity dependent on the Re number, inlet temperature of 35 $^{o}$C, and outflow at the outlet.

Table III-5 shows the heat transfer coefficient, h, computed with the high-Re model and the correlations. At Re=70000 the high-Re model predicts a heat transfer coefficient that is 4% lower than hp. At higher Re number values the high-Re model predicts a heat transfer coefficient that is 6% higher than hp. The predictions of the Dittus – Boelter correlation are up to 16% lower than those of the Petukhov correlation. The predictions of the modified Dittus – Boelter correlation are up to 9% lower, and those of the Sieder-Tate correlation up to 8% higher than $h_p$.

Table III-5. BR2 Plate Geometry: Variable Properties - High-Re model vs Correlations

| Re = 70009, Pr = 2.6776, $\mu_w/\mu_b$ = 0.535 | | |
|---|---|---|
| Method | h | $h/h_p$ |
| High-Re model | 32234 | 0.961 |
| Dittus – Boelter | 29300 | 0.874 |
| Dittus – Boelter-M | 31387 | 0.936 |
| Sieder – Tate | 35157 | 1.049 |
| Petukhov | 33529 | |
| Re = 99976, Pr = 2.1629, $\mu_w/\mu_b$ = 0.537 | | |
| Method | h | $h/h_p$ |
| High-Re model | 43579 | 1.063 |
| Dittus – Boelter | 36483 | 0.890 |
| Dittus – Boelter-M | 39065 | 0.953 |
| Sieder – Tate | 44381 | 1.083 |
| Petukhov | 40996 | |
| Re = 141896, Pr = 2.1623, $\mu_w/\mu_b$ = 0.523 | | |
| Method | h | $h/h_p$ |
| High-Re model | 58394 | 1.062 |
| Dittus – Boelter | 48273 | 0.878 |
| Dittus – Boelter-M | 51844 | 0.943 |
| Sieder – Tate | 58946 | 1.072 |
| Petukhov | 54965 | |
| Re = 199838, Pr = 2.3049, $\mu_w/\mu_b$ = 0.517 | | |
| Method | h | $h/h_p$ |
| High-Re model | 80005 | 1.057 |
| Dittus – Boelter | 64971 | 0.858 |
| Dittus – Boelter-M | 69855 | 0.923 |
| Sieder – Tate | 79112 | 1.045 |
| Petukhov | 75701 | |
| Re = 306148, Pr = 2.3030, $\mu_w/\mu_b$ = 0.501 | | |
| Method | h | $h/h_p$ |
| High-Re model | 114934 | 1.057 |
| Dittus – Boelter | 91368 | 0.841 |
| Dittus – Boelter-M | 98588 | 0.907 |
| Sieder – Tate | 111768 | 1.028 |
| Petukhov | 108705 | |

As shown in Table III-6, the v2f model predicts an $h$ value that is up to 9% higher than $h_p$. The predictions of the correlations shown in Table III-6 are slightly different than those of Table III-5 because the Re values and the values of $\mu_w/\mu_b$ are slightly different.

Table III-6. BR2 Plate Geometry: Variable Properties - v2f model vs Correlations

| Re = 69998, Pr = 2.2696, $\mu_w/\mu_b$ = 0.538 | | |
|---|---|---|
| Method | h | $h/h_p$ |
| v2f model | 33012 | 1.055 |
| Dittus – Boelter | 27914 | 0.892 |
| Dittus – Boelter-M | 29884 | 0.955 |
| Sieder – Tate | 33840 | 1.082 |
| Petukhov | 31287 | |
| Re = 95913, Pr = 2.2695, $\mu_w/\mu_b$ = 0.527 | | |
| Method | h | $h/h_p$ |
| v2f model | 43331 | 1.065 |
| Dittus – Boelter | 35913 | 0.883 |
| Dittus – Boelter-M | 38538 | 0.948 |
| Sieder – Tate | 43667 | 1.074 |
| Petukhov | 40669 | |
| Re = 140315, Pr = 2.1986, $\mu_w/\mu_b$ = 0.511 | | |
| Method | h | $h/h_p$ |
| v2f model | 59864 | 1.087 |
| Dittus – Boelter | 48132 | 0.874 |
| Dittus – Boelter-M | 51823 | 0.941 |
| Sieder – Tate | 58897 | 1.070 |
| Petukhov | 55062 | |
| Re = 197433, Pr = 2.3491, $\mu_w/\mu_b$ = 0.507 | | |
| Method | h | $h/h_p$ |
| v2f model | 82689 | 1.092 |
| Dittus – Boelter | 64702 | 0.854 |
| Dittus – Boelter-M | 69724 | 0.920 |
| Sieder – Tate | 75748 | 1.042 |
| Petukhov | 78912 | |

## *III.4. Summary and conclusions*

### III.4.1. Summary for low-Re and v2f models

For constant properties and pipe flow, among the three correlations the Dittus-Boelter correlation predicts the lowest heat transfer coefficient. There is a better agreement between predictions of the Sieder-Tate and those of the Petukhov correlation. At the low Re value considered in this analysis(Re=66112), the low-Re model predicts the smallest value of $h$. There is a good agreement between predictions of the CFD models and the correlations, especially Sieder-Tate and Petukhov at Re=132000. At Re close to 200000, the predictions of the CFD models are significantly higher than those of the correlations, while those of the correlations are in quite good agreement.

For variable properties, the Dittus-Boelter correlation predicts the smallest $h$ value. The modified Dittus-Boelter correlation predicts lower values than the Petukhov correlation but the agreement is within 6% in pipe flow and 9% in the flow between plates. The predictions of the Sieder-Tate correlation are higher than those of Petukhov, but the maximum difference is about 10% in pipe flow and 8% in the flow between plates.

For pipe flow, at the low Re value of 67000 the low-Re model predicts an $h$ value 10% lower than the Petukhov correlation, while the prediction of the v2f model is in very good agreement with that of the Petukhov correlation. As the Re number increases, both CFD models predict higher $h$ values than the Petukhov correlation, about 20% higher at Re numbers greater than 140,000, while their predictions are in a good agreement with each other. For flow between plates, the v2f model predicts an $h$ value that is up to 9% higher than $h_p$.

### III.4.2. Summary for standard high Reynolds number $k-\varepsilon$ model

The predictions of standard high Reynolds number $k-\varepsilon$ model agree quite well with those of the Petukhov correlation. For pipe flow and constant properties they are consistently about 7% lower than $h_p$. For variable properties they are consistently up to 6% higher than $h_p$. For flow between plates and variable properties, at Re=70000 they are 4% lower than $h_p$, and at higher Re number values they are 6% higher.

### III.4.3. Conclusions

Based on the comparisons with experimental data for pipe flow presented in Refs [6] and [9], and for the Re number range covered in these comparisons, the heat transfer coefficient is underpredicted by the Dittus-Boelter correlation and overpredicted by the Sieder-Tate correlation. The predictions of the Petukhov correlation agree better than the other correlations with the experimental data for pipe flow, up to Re =123000, and for higher Re values are more

conservative than those predicted by the CFD models (for both pipe flow and flow between plates). Based on the analysis presented in Part III, the Petukhov correlation seems to be a better choice for the safety margin analysis (OB or ONB). A less conservative choice than the Dittus-Boelter correlation, and a little more conservative than the Petukhov correlation, would be the modified Dittus-Boelter correlation, which accounts for the variation of viscosity with temperature.

The discrepancies between correlations and CFD models depend on both, the Re number and the Prandtl number. There is a need of comparison with experimental data to determine whether the CFD models provide more accurate predictions than the correlations. The experimental data of Ref. [6] does not exceed a Re value of 123000, and that used in Ref. [8] does not exceed a Re value of 100000.

## References


[1] Arne P. Olson and M. Kalimullah, "A Users Guide to the PLTEMP/ANL v4.1 code," ANL/RERTR/TM-11/22, Revision 0, Argonne National Laboratory, 2011.

[2] RELAP5-3D Code Development Team, "RELAP5-3D Code Manual," INEEL-EXT-98-00834, 2005.

[3] STAR-CD Version 3.20, CD-adapco Group, New York, 2004.

[4] S. Kalcheva, E. Koonen, B. Dionne, C. Tzanos, A. Olson, M. Kalimullah, E. Feldman, "Preliminary Evaluation of Safety Margins of HEU and LEU BR2 cores", SCK•CEN Report, BLG-1079, 12 December, 2010.

[5] B. Dionne and C.P. Tzanos, "Estimation of Steady State and Transient Power Distributions for the RELAP Transient Analysis of the 1963 Loss of Flow Tests at BR2," ANL/RERTR/TM-11/19, Argonne National Laboratory, 2011.

[6] J. P. Hartnett and T. F. Irvine, Jr, Editors, "Advances in Heat Transfer," Vol. 6, Academic Press, New York, 1970.

[7] D. B. R. Kenning, R. A. W. Shock, and J. Y. M. Poon, " Local Predictions in Heat Transfer Due to Buoyancy Effects in Upward Turbulent Flow," Heat Transfer 1974, Fifth International Heat Transfer Conference, Japan, September 3-7, 1974, Vol. III, p. 139.

[8] J. H. Fertziger and M. Peric, "Computational Methods for Fluid Dynamics," Springer-Verlag, 1997.

[9] C. A. Sleicher and N. W. Rouse, "A Convenient Correlation for Heat Transfer to Constant and Variable Property Fluids in Turbulent Pipe Flow," Int. J. Heat Mass Transfer, Vol. 18, pp677-683, 1975.

**Nuclear Engineering Division**
Argonne National Laboratory
9700 South Cass Avenue, Bldg. 208
Argonne, IL 60439-4842

www.anl.gov

Argonne National Laboratory is a U.S. Department of Energy
laboratory managed by UChicago Argonne, LLC